Carbon fibers/nickel nanocomposite particles reinforced ethylene vinyl acetate stretchable conductive polymer: fabrication, microstructure, electrical and mechanical properties.

DAOUSH, W.M., AL-ZUAIR, A.F., SAHARUDIN, M.S. and INAM, F.

2024

ORIGINAL ARTICLE

Carbon fibers/nickel nanocomposite particles reinforced ethylene vinyl acetate stretchable conductive polymer: fabrication, microstructure, electrical and mechanical properties

Walid M. Daoush[1,2] Abdullah Fahad Al-Zuair[1] Mohd Shahneel Saharudin[3] Fawad Inam[4,5]

Abstract

Carbon fibers of polyacrylonitrile (PAN) type were coated with nickel nanoparticles using a chemical reduction method in alkaline hydrazine bath. The carbon fibers were firstly heated at 400 °C and then chemically treated in hydrochloric acid followed by nitric acid to clean, remove any foreign particles and functionalized its graphitic surfaces by introducing some functional groups. The functionalized carbon fibers were coated with nickel to produce 10 wt% Cf/Ni nanocomposites. The uncoated heat treated and the nickel coated carbon fibers were investigated by SEM, EDS, FTIR and XRD to characterize the particle size, morphology, chemical composition and the crystal structure of the investigated materials. The nickel nanoparticles were successfully deposited as homogeneous layer on the surface of the functionalized carbon fibers. Also, the deposited nickel nanoparticles have quazi-spherical shape and 128–225 nm median particle size. The untreated and the heat treated as well as the 10 wt% Cf/Ni nanocomposite particles were further reinforced in ethylene vinyl acetate (EVA) polymer separately by melt blending technique to prepare 0.5 wt% Cf-EVA polymer matrix stretchable conductive composites. The microstructures of the prepared polymer composites were investigated using optical microscope. The carbon fibers as well as the nickel coated one were homogenously distributed in the polymer matrix. The obtained samples were analyzed by TGA. The addition of the nickel coated carbon fibers to the EVA was improved the thermal stability by increasing the thermal decomposition temperature T_{max1} and T_{max2}. The electrical and the mechanical properties of the obtained 10 wt% Cf/Ni nanocomposites as well as the 0.5 wt% Cf-EVA stretchable conductive composites were evaluated by measuring its thermal stability by thermogravimetric analysis (TGA), electrical resistivity by four probe method and tensile properties. The electrical resistivity of the fibers was decreased by coating with nickel and the 10 wt% Cf/Ni nanocomposites has lower resistivity than the carbon fibers itself. Also, the electrical resistivity of the neat EVA is decreased from 3.2×10^{10} to 1.4×10^{4} Ω cm in case of the reinforced 0.5 wt% Cf/Ni-EVA polymer composite. However, the ultimate elongation and the Young's modulus of the neat EVA polymer was increased by reinforcing with carbon fibers and its nickel composite.

Keywords Carbon fibers · Nickel nanocomposites · EVA · Stretchable conductor polymer · Tensile properties

1 Introduction

Synthesis and characterizations of carbon fibers (Cfs) and its composites are considered as rapidly developing industrial field due to the combination of lightness, high abrasion resistance and low thermal shrinkage and expansion coefficient, superior strength/weight ratio, and good electrical properties. These unique properties impregnate these types of materials in different applications such as supercapacitors, sports goods, bio-medical, electromagnetic shielding interference (EMI) shielding materials in airplane, airspace structural parts, wind turbine blades and building of thanks [1–3].

Carbon fibers can be classified into polyacrylonitrile (PAN), pitch, and viscose-based CFs according to the source of the precursor [4]. Different physical or chemical approaches have been explored for depositing metals on carbon nano fibers and nanotubes to improve its mechanical properties [5]. These methods involve hard coatings of the carbon fibers by different techniques such as physical vapour deposition (PVD) [6, 7], chemical vapour deposition (CVD) [8], electroless plating [9] and the electrochemical

deposition of metals such as copper on the surface of the carbon fibers [10]. Other physical and chemical methods were also explored such as chemical reduction process, thermal treatment, hydrothermal or solvo-thermal and self-assembly processes [5, 11]. By using such metallic additives, it is possible to obtain carbon fiber reinforced polymer composites (CFRPs) materials suitable for different new applications. However, there are some drawbacks to the properties of such fiber reinforced polymer composites seriously effect on the overall performance of the composite include brittleness of the matrix and weak interfacial bonding between the fiber and the polymer matrix [12, 13]. Thermosetting and thermoplastic resins can be used usually as polymer matrix. The thermosetting resins include epoxy, polyimide and phenolic resins. On the other hand, the thermoplastic resins include polyethylene, nylon, polytetrafluoroethylene and polyetheretherketone [14].

Carbon fibers are characterized by a non-polar, inert, relatively smooth surface and weak wettability toward different types of polymers [15], leading to delamination and low mechanical strength of the polymer composites [16]. Many techniques have been developed to improve the wettability between the CFs and the polymer matrix. One possibility of achieving suitable adhesion at the interface, enabling the transfer of loads in a polymer–fiber interface, is to apply sizing agent on the surface of the carbon fibers or depositing coating layers on the surface of the carbon fibers [17–19] or graphene [20, 21]. The mechanical properties of the CFRP composites can be improved by enhancing the interfacial bonding strength between the CFs and the polymer matrix keeping of the desired interfacial microstructure and chemical composition, therefore, it is essential to conduct detailed research on the interfacial properties [22, 23]. However, the loss of the electrical conductivity owing to the polymer matrix reduces its performance of its specific application. One of the solution of this problem is the metallization process by applying a conductive metallic layer on the surface of the CFs using electroless or electrochemical deposition, chemical vapor deposition and physical vapor deposition. A different route proposed for CFs/metal/polymer adhesion enhancement by introducing some functional groups, such as –OH and –COOH on the graphitic structure of the Cfs [24, 25].

Chemical reduction process is used to deposit different types of nanoparticles composed mainly of palladium, silver and copper metals on different carbon and other materials using different reducing agents [9, 10, 26–28]. Synthesis of nickel and its nanocomposites with different metals was also studied by using sodium borohydride [26] and sodium hypophosphite [29] as reducing agents. It was reported in previous work that the metal nanoparticles as well as metallic nanocomposites can be deposited in aqueous solutions under room pressure on different types of substrates by adjusting the optimum temperature of the process [9, 10].

EVA is an important class of thermoplastics copolymer used for different applications such as coating, foaming, adhesives, biomimetic materials, and synthetic leathers due to their useful properties such as excellent flexibility, elasticity, and damping ability. Despite the fact that EVA copolymers have unique properties, their high flammability, low tensile strength, and relatively weak thermal stability decrease its performance and applications [30]. For this reason, many efforts were done to solve this problem as much as possible [31]. To obtain an efficient flame retardant material, high loading of carbon fibers is required which results in sacrificing the mechanical properties [32, 33].

Materials composed of EVA reinforced by carbon fibers are candidate materials can be used in different applications such as fabrications of stretchable conductors and electromagnetic interference shielding (EMI) materials [34]. Stretchable conductors and electromagnetic interference materials are essential assembly units of next-generation flexible electronics, requiring good electrical conductivity, electromagnetic shielding and stretchability simultaneously. The poor interfacial adhesion between conductive reinforcements such as Cfs and the polymer matrix often deteriorating the final conductivity [35, 36]. The use of EVA copolymer without additives features some drawbacks involving low electrical and thermal conductivity and sometimes inadequate mechanical properties. It was reported in previous work that; the properties of the polymer can be improved by the impregnation of some metallic, metal oxides or inorganic nanoparticles in the polymer matrix due to the dispersion and the local interactions between the matrix and the nanoparticles, lead to improvement of its physical and mechanical [37]. Also, the combination of pure EVA with conductive reinforcements such as graphene-based or metals-based materials can increase its electrical conductivity and EMI shielding efficiency, but they suffer from low flexibility and poor mechanical properties [35, 38]. Reinforcement particles such as metals, graphite, carbon nanotubes, carbon blacks, and carbon fibers are used in polymer matrix to enhance the conductivity and EMI shielding property [39, 40]. Fortunately, carbon fibers can impregnate effective conductive networks in a polymer matrix due to its good electrical conductivity and EMI shielding properties [41, 42].

In the present work, carbon fibers/EVA as well as Carbon fibers-Ni/EVA composites were prepared by the combination of the EVA polymer with the carbon fiber in order to fabricate new polymer matrix composite materials with good thermal stability, mechanical and electrical properties and improving its performance as stretchable conducting as well as EMI material. The process steps started by the heat and acid functionalization of carbon fibers followed by coating with nickel nanoparticles using an alkaline hydrazine bath. The uncoated and the heat-treated as well as the nickel coated Cfs composites were reinforced in EVA polymer

matrix by melt blending technique to produce the Cfs/EVA polymer matrix composites. The microstructure, thermal stability and the physical as well as the mechanical properties of the obtained composites were measured to study the enhancement of the interfacial bonding and the adhesion between the nickel coated carbon fibers and the EVA polymer matrix and its effect on its performance.

2 Materials and methods

2.1 Materials

Bobbin of PAN-Type carbon fibers was purchased from Mitsubishi chemicals, Japan. Table 1 lists the characteristics and the properties of the carbon fibers under investigations. All reagents used in the synthesis processes are analytically grade. Nickel sulphate hexahydrate (Winlab LTD Co., UK), Hydrazine hydrate (Loba Chemi., Mumbai), Sodium hydroxide solid pellets (Panreac Co., EU).

2.2 Methods

2.2.1 Surface treatments and functionalization of carbon fibers

The investigated carbon fibers are heat treated at 400 °C for 30 min in an oven to remove any volatile compounds of the binding agent which is added during the fabrication processes of the carbon fibers. The heat-treated fibers are washed with 20 mL acetone for 15 min to dissolve any remained organic impurities and then dried in air. The obtained carbon fibers were undergoing Ultrasonication at 40 kHz for 5 h in (1:3 volume %) HCl solution to dissolve any inorganic impurities contaminated its surfaces. The cleaned carbon fibers were chemically treated by acid functionalization using 15 mL of concentrated (67%) Nitric acid. The obtained carbon fibers were washed several times with distilled water to remove any remaining acid, dried and stored for further investigations.

Table 1 Properties of the PAN carbon fibers used in the study

Property	Value
Density, g cm^{-3}	1.78
Diameter, μm	7
Filament count	1000
Purity	> 90%
Specific heat, J kg^{-1} K^{-1}	711
Electrical resistivity, Ω cm	2.2×10^{-3}
Thermal conductivity. W m^{-1} K^{-1}	8
Tensile strength, GPa	3
Tensile modulus, GPa	221
Ultimate elongation, %	1.4

2.2.2 Synthesis of Cf-Ni Nanocomposites

Nickel sulphate hexahydrate (1 g) was dissolved in 50 mL of distilled water under magnetic stirring at a speed of 350 rpm for 15 min. Calculated amount of the obtained acid treated carbon fibers (89 mg) is added to the above prepared mixture and stirred by magnetic stirrer at 500 rpm. A combined reducing mixture consists of sodium hydroxide (500 mg) and 19 mL of hydrazine hydrate solution (80 volume %) at pH of 12.5 is prepared. Then, the freshly prepared reducing mixture is added dropwise to a hot solution of the prepared nickel sulphate/carbon fibers mixture at ~ 67 °C until the reaction was completed within ~ 30 min. The obtained carbon fibers/nickel (Cfs/Ni) nanocomposite powder is extensively washed with distilled water then dried and stored for further investigation. Figure 1 illustrates a Schematic diagram of the synthesis process setup of Cf/Ni nanocomposite.

2.2.3 Fabrication of CF/Ni-EVA polymer composites

The untreated, heat treated and 10 wt% Cf/Ni nanocomposites are used to prepare 0.5 wt% Cf/EVA, 0.5 wt% Cf_t/EVA and 0.5 wt% Cf/Ni-EVA polymer matrix composites. Figure 2 illustrates a schematic flowchart of the synthesis process of Cf/Ni-EVA polymer matrix nanocomposite.

The carbon fibers volume fraction (V_f) of the composites is calculated by a simple approximation to the theoretical value of the carbon fibers volume fraction according to the rule of mixtures, as depicted in Eq. (1):

$$V_f = \frac{w_f \times \rho_m}{w_f \times \rho_m + w_m \times \rho_f} \quad (1)$$

where w_f is the weight of the fibers, w_m is the weight of the matrix, ρ_f is the density of the fibers, and ρ_m is the density of the EVA matrix. By using the above-mentioned equation, it is obtained that the calculated volume fraction corresponding to 0.5 wt% of the carbon fibers is equivalent to 0.3 Volume % by considering the EVA density of 1.01 g/cm^3 and the density of carbon fibers is 1.78 g/cm^3.

2.2.4 Characterizations and microstructure investigations

The acid functionalized carbon fibers was investigated by FTIR spectrophotometer of model Bruker TENSOR; Germany. The untreated and heat treated as well as the nickel coated carbon fibers underwent sputtered with platinum before scanning and then the sputtered samples were investigated using Field Emission Scanning Electron Microscopy of model JEOL, JSM-7600F connected

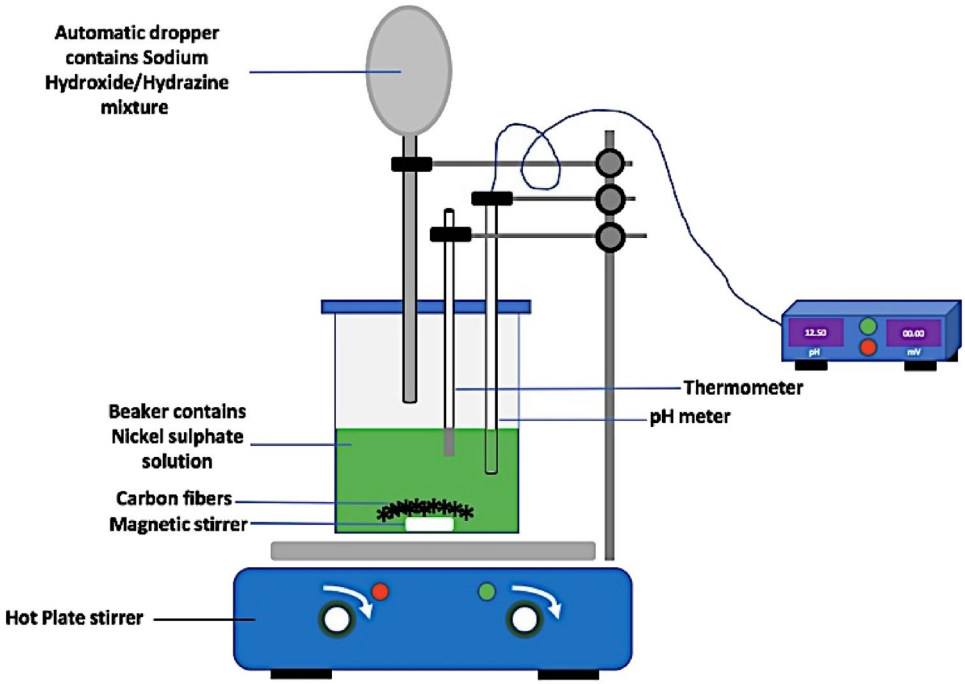

Fig. 1 Schematic diagram of the synthesis process setup of 10 wt% Cf/Ni nanoparticles

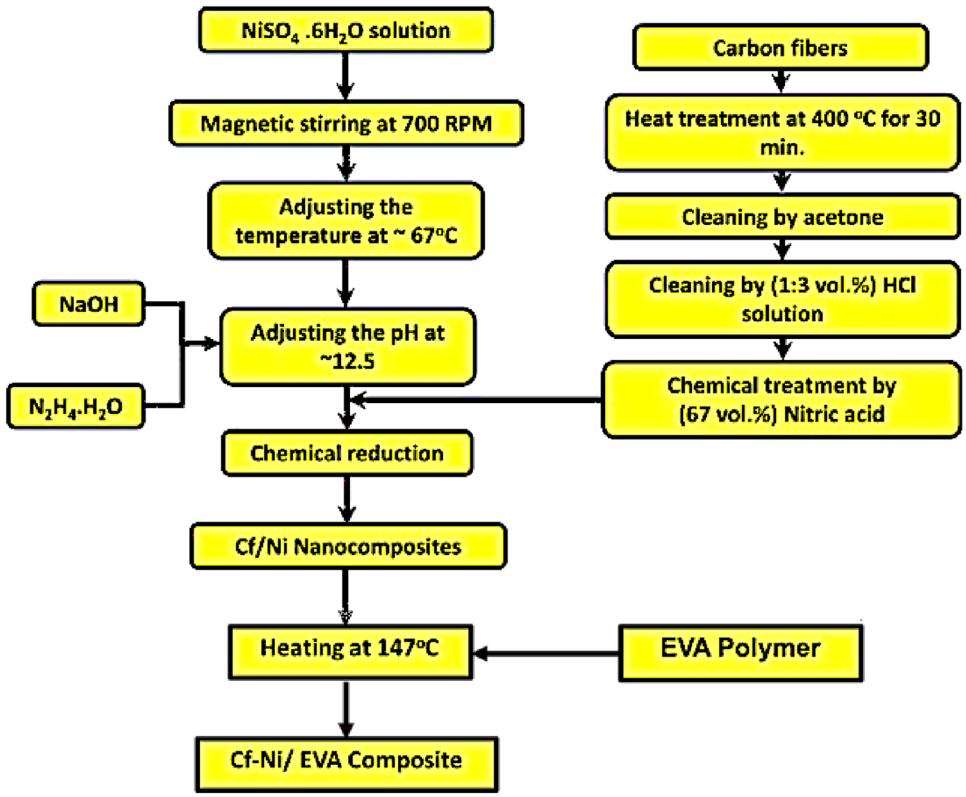

Fig. 2 Schematic flowchart of the synthesis process of 10 wt% Cf/Ni nanoparticles and its composite with EVA polymer

with EDS analysis unit. In addition, the investigated samples underwent crystalline phase analysis using XRD Brucker D8 discover model. The micrographs of the prepared 0.5 wt% Cf/EVA, 0.5 wt% Cf_t/EVA and 0.5 wt%

Cf/Ni-EVA composites were investigated using optical microscope.

2.2.5 Thermogravimetric analysis (TGA)

The produced samples are investigated by TGA analysis to determine its decomposition temperature and the weight loss percentage was also determined. Thermogravimetric analysis (TGA) was carried out utilizing a TGA-Q600 machine from TA Instrument, New Castle, DE, USA. The samples were put in alumina crucible, and thermal analysis was carried out in a nitrogen (N_2) environment from 25 to 1000 °C at a rate of 10 °C/min.

2.2.6 Electrical resistivity measurements

The electrical resistivity of the untreated, heat treated carbon fibers, the prepared 10 wt% Cf/Ni nanocomposites as well as the neat EVA and the 0.5 wt% Cf/Ni-EVA stretchable conductive composite were measured using ohmmeter device. A fixed direct current (DC) was passed through the test specimen via crocodile clips. The dimensions of the fibers were then calculated. Each bundle was composed of around 1000 filaments of diameter ~ 7 μm and a length ~ 6 cm. For each test, the ohmmeter was zeroed with no current passing through the specimen, and then the measurement is carried out. The resistivity (ρ) in μΩ cm was calculated according to the following equation

$$R = (\rho \cdot L)/A \tag{2}$$

where R is the resistance in Ω, L is the measured length in cm, A is the cross-section area in cm^2.

2.2.7 Tensile test measurements

The tensile properties of the fabricated neat EVA, 0.5 wt% Cf/EVA, 0.5 wt% Cf_t/EVA and 0.5 wt% Cf/Ni-EVA composites underwent tensile test by using tensile machine of model INSTRON-5984. The scan rate of the load/displacement is adjusted during the test at 10 mm/min. The dimensions of the specimens and experimental methods of the tensile test were based on the ASTM D 638 standard.

3 Results and discussion

3.1 Surface treatments and acid functionalization of the carbon fibers

The first step of the treatment process of the as received carbon fibers is the removing of any volatiles and organic materials such as binding and sizing agents which added to the fibers during the fabrication process. It was found that the optimum heating conditions are at moderate temperature of 400 °C for 30 min avoid dissociation at high temperature. The obtained fibers were then subjected to acid functionalization by concentrated HNO_3 to introduce functional groups such as carbonyl and/or carboxylic groups on the graphitic surface which improve the electroless nickel deposition on the surface of the carbon fibers [9, 10].

The functionalization process expected to modifies the surface of the carbon fibers which leads to the breakdown of the –C=C bond in the graphitic backbones. As reported from the literatures for the functionalization of the carbon allotropies like fullerenes, CNTs and carbon fibers. The introduction of oxygenated groups like hydroxyl or carboxylic groups into the graphitic structure enhances the formation of a uniform coating layer on its surface [43]. It was also reported in the literature that a number of functionalization methods have been studied to address different application requirements of functionalizing carbon fibers [44]. In the current study, chemical oxidation method of the surface of the carbon fibers by HNO_3 is improved, the addition of surface polar functional groups effectively increases surface wettability of fibers, and the chemical oxidation using strong oxidizing acids is easier to obtain more carboxyl groups than the others. FTIR spectrum is presented in Fig. 3. It was revealed that; the infrared spectrum indicates several characteristic bands. The first type of bands are C–O stretching mode of alcohol and phenol at 1100 and 1029 cm^{-1}, respectively. The second one is a broad band appeared at around 3142–3477 cm^{-1} which is the stretching mode of hydrogen-bond of the hydroxyl O–H groups of the carboxylic acid, alcohol, and phenol. The third type of functional groups is the C=C bond and C=O, which are detected as stretching mode at 1637 cm^{-1}, indicating the graphitic backbone structure of the carbon fibers. The forth one of bonding is the C-H bond in the aldehyde CHO group, which appeared as stretching mode at 2916 cm^{-1} and 2848 cm^{-1} [45–49]. The fifth type of band comes from the phenyl ring and is observed at 613 cm^{-1}. The band (1151 cm^{-1}) of the sixth type of functional group can be assigned to the C–O–C band. The seventh type of bands detected at 1417 cm^{-1} and 1458 cm^{-1} due to the O–H of the carboxylic and N–O of the nitro groups remained from the functionalization by nitric acid, respectively. The last type of band was detected at 1103 cm^{-1}. It can be assumed from the comparison of the band intensities that hydroxyl groups are the more dominant group which introduced on the graphitic structure of the carbon fibers than the carboxyl, aldehyde, and ether groups due to the functionalization process by nitric acid. It was reported in the literatures for the functionalization of carbon fibers by introducing hydroxyl groups on its graphitic structure appears to be the key of the enhancement of the formation of a uniform coating layer on its surface which

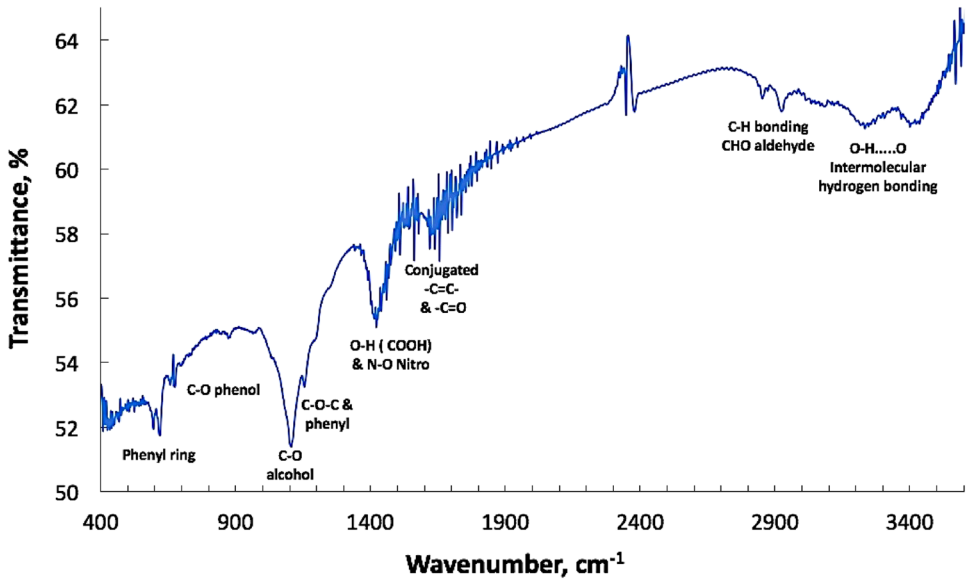

Fig. 3 FTIR spectrum of the functionalized carbon fibers by HNO_3

expected improve the properties and the adhesion between the carbon fibers and the coating layer [50, 51].

Groups containing nitro and oxide were present on the surface of carbon fibers as intermediate products of functionalization (Fig. 4). These intermediates were also present on the surface of carbon fiber and then transformed to the –OH bond. The –OH bond and C–O can be further oxidized to –COOH. Once the HO–C–OH bond was formed, the functional group rapidly transformed into C=O and a carboxyl group. Functionalization was accompanied by fracture of the C=C bond. The turbostratic carbon determined the strength of carbon fibers, and the fracture of C=C bonds largely degraded the tensile strength of carbon fibers [52, 53].

Figure 5a, b shows the SEM images with low and high magnifications of the uncoated carbon fibers. It was observed that, the surface of the carbon fibers was contaminated with different particles of impurities. The EDAX compositional analysis presented in Fig. 5c, d shows the elemental analysis of this impurities are mainly composed of Cr, Ba and O. Figure 5e, f shows SEM images of the treated carbon fibers after acid functionalization. The results revealed that the surface of the functionalized carbon fibers is cleaned due to the heat and the acid treatments which removing the different particles and impurities of the binding agents attached to the surface. Also, it was observed that, the functionalized carbon fibers have rough surface which expect to improve the coating process with nickel nanoparticles (see Fig. 5f).

3.2 Fabrication and characterization of Cf/Ni nanocomposites

Deposition of nickel nanoparticles on the surface of the treated carbon fibers have been studied under the controlling of reaction conditions. The minimum components of a solution are a salt of nickel such as nickel sulphate hexahydrate and a reducing agent such as hydrazine hydrate. The chemical solution utilized hydrazine as a reducing agent, the pH of the solution should be adjusted between 12 and 13 and the temperature between 70 and 90 °C.

It was observed from the results that; the rate of the addition of the hydrazine reducing agent to the reaction mixture is effect on the deposition process of nickel on the surface of the carbon fibers. When the rate of addition of hydrazine is very fast the reaction can be completed within few minutes, however, the addition of the hydrazine is controlled then the deposition of the nickel nanoparticles on the surface of the carbon fibers will be slower. The deposition of the nickel on the surface of carbon fibers

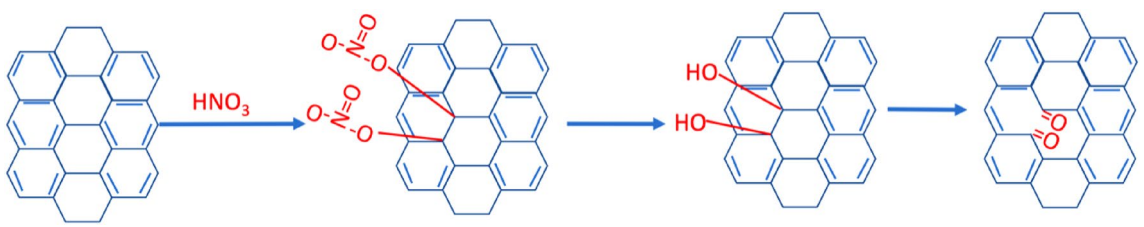

Fig. 4 Oxidation process on the surface of the graphitic structure of carbon fibers

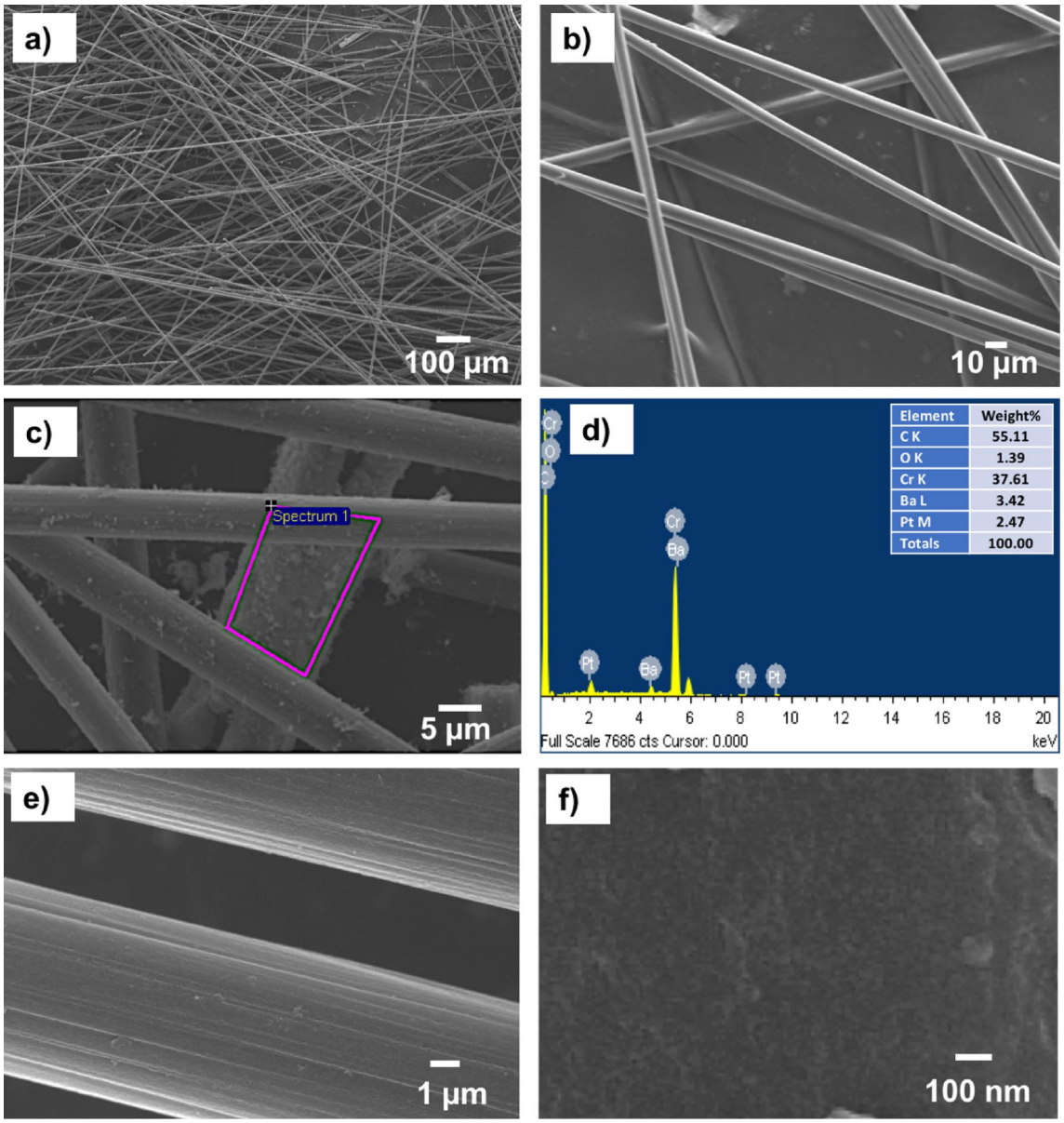

Fig. 5 SEM images with different magnifications and EDAX analysis of **a**, **b** of as received carbon fibers, **c**–**e** heat treated carbon fibers at 400 °C for 30 min, **f** acid functionalized carbon fibers (Pt peak, is the background of the sputtered process)

is an autocatalytic reaction. The carbon fibers can act as autocatalytic conductive surfaces which can enhance the oxidation–reduction reaction between the nickel ions and the hydrazine hydrate [N_2H_5OH] reducing agent. Also, the deposition process of nickel nanoparticles is affected by the presence of functional groups such as –COOH or –OH on the carbon fibers substrate surface and on the nucleation (seed formation) during the initial steps of the process, when the nucleus particles is very fine; the deposition reaction is very slow due to the large surface area of the nucleus [54–56]. It was also reported in previous reports that; the reaction process is sensitive to the molar ratio of [N_2H_5OH]/[Ni^{2+}] and the reaction temperature. Consequently, the presence of excess hydrazine hydrate in the solution participated in the decomposition reaction of the complexes which can be formed between nickel and hydrazine. From the above observations, it is expected that even after the formation of the hydrazine complexes, the solution still contained free hydrazine, which could influence on the reduction reaction in the later stages of the deposition of the nickel nanoparticles on the surface of the carbon fibers. As soon as the [N_2H_5OH]/NaOH mixture was added to the solution which containing nickel hydrazine complexes, the color of the solution slowly changed

to dark brown, indicating the formation of the nuclei of nickel nanoparticles on the surface of the carbon fibers. As time progresses and the consumption of $[N_2H_5OH]$/NaOH reagents is increased, all the nickel ions in the solution were reduced to metallic nickel in the form of nickel nanoparticles on the surface of the carbon fibers. The synthesis process of nickel nanoparticles is proceeded according to the following oxidation–reduction reaction [55, 56];

$$2Ni^{2+} + 4OH^- + N_2H_4 \rightarrow 2Ni + N_2 + 4H_2O \quad (3)$$

By applying of the Nernst equation on the reaction (3) by considering the reaction as oxidation reduction reaction and the number of electrons transferred in the reaction is ($n = 4$); we can obtain the Eq. (4) and we can express the effect of the temperature and the $[OH^-]$ on the reaction.

$$\Delta E = E_o - 2.303\,(RT/4F)\,\log\,(1/[OH^-]) \quad (4)$$

It is obvious that either increasing temperature, or increasing the $[OH^-]$ by the addition of NaOH leading to increase of ΔE of the reaction and according to the relationship (4) between the Gibbs free energy ΔG and the ΔE; the reaction will be more spontaneous and higher number of nuclei and thereby formation of smaller nanoparticles in size will be predominant [56]

$$\Delta G = -nF\Delta E \quad (5)$$

High-resolution scanning electron microscope images with low and high magnifications and EDAX compositional analysis of the prepared nickel coated carbon fibers are shown in Fig. 6a–e. It was observed from the results that; thin, homogeneous and uniform layer of nickel was deposited on the surface carbon fibers. Also, the size of the deposited nickel nanoparticles on is very fine of 128–225 nm median particle size. Also, the deposited nickel nanoparticles have quazi-spherical particle shape and some agglomerated particles can be observed. The EDAX compositional analysis (see Fig. 6e) revealed that the nickel coated carbon fibers are composed mainly of nickel and carbon. The small intense peak is also detected due to the presence of the oxygen element by the formation of some nickel oxides during the electroless process in solutions and drying of the powder in air atmosphere.

According to our preliminary studies, it was observed that; the deposition of 10 weight % of nickel nanoparticles layer on the carbon fibers are enough to complete encapsulating the surface of the carbon fibers by homogeneous, thin and uniform nickel layer. However, by increasing the nickel content more than 10 weight % (the preliminary study conducted up to 25 weight % of nickel), loosely

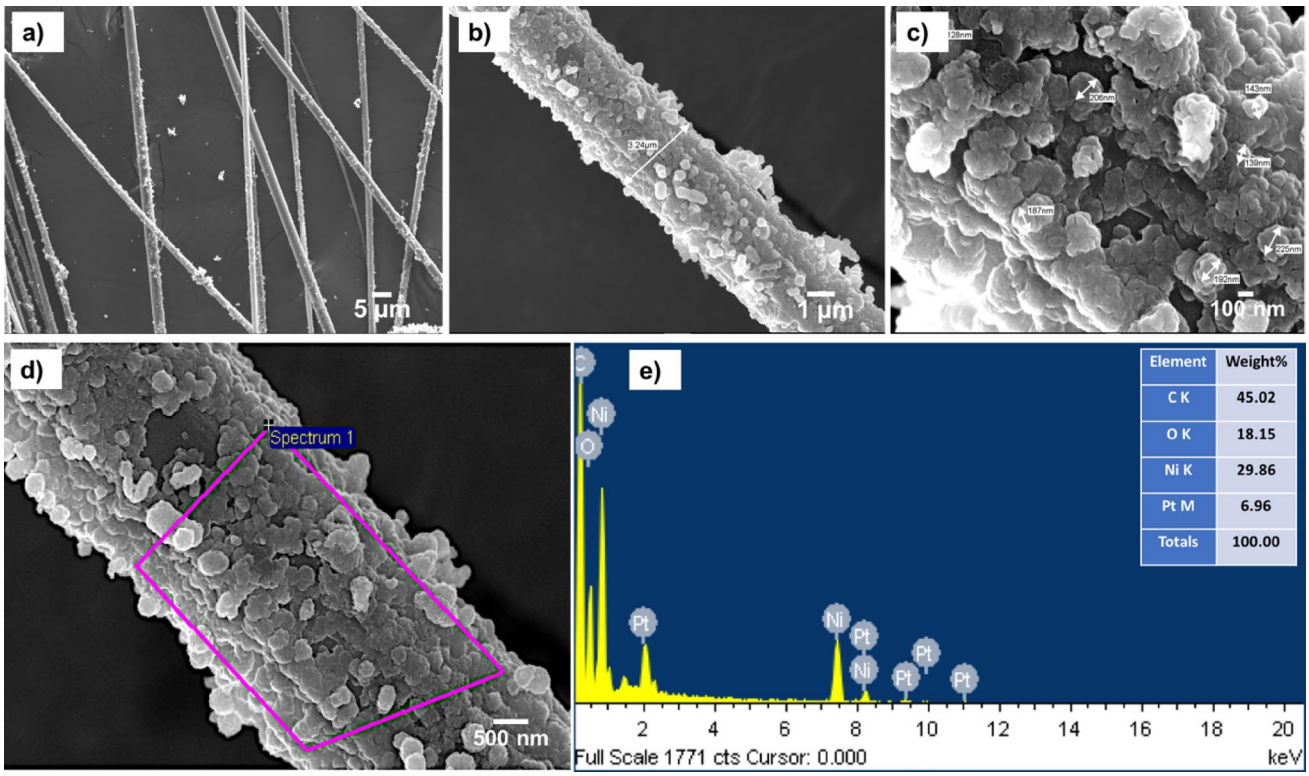

Fig. 6 SEM images of **a** carbon fibers, **b** 10 wt% carbon fibers/Ni nanocomposites, **c**, **d** EDAX compositional analysis of the 10 wt% carbon fibers/Ni nanocomposites prepared by the electroless deposition method (Pt peak, is the background of the sputtered process)

bonded multilayers of nickel nanoparticles are deposited on the carbon fibers and can be detached from the surface of the carbon fibers forming some fragments of the Cf/Ni nanocomposites and loosely bonded nickel nanoparticles. The reason behind that is the difference in the densities between the deposited nickel and the carbon fibers. Also, the difference in the thermal expansion coefficient between the nickel layer and carbon fibers which are expanded during the drying and the melt blend fabrication process later [29]. Due to these reasons, it was preferred to deposit thin layer of 10 weight % nickel instead of thick layer one on the surface of the carbon fibers to retain the continuity of the carbon fibers in the Cf/Ni nanocomposite helping in conducting the electricity and enhance the mechanical properties.

Figure 7 shows the XRD patterns of the synthesized carbon fibers/Ni nanocomposites. The specific diffraction peaks (111), (200), and (220) are corresponding to the presence of the fcc structure of metallic nickel phase. These diffraction peaks are in agreement with JCPDS No. 04-0850 [29]. In addition, the low three intense peaks (010), (012) and (110) are corresponding to the hcp nickel phase in agreement with JCPDS No. 45-1027 [55]. However, the diffraction peaks (111), (200), (220), (311) and (222) are associated with the presence of the fcc nickel oxide in agreement with JCPDS No. 04-0835 [55]. Also, low intense peak at 2 theta of 20° is appeared due to the presence of the carbon fibers dispersed in the carbon fibers/Ni nanocomposites [9, 10]. This indicated that the deposited nanoparticles on the surface of the carbon fibers are composed mainly of NiO/Ni phase [55].

3.3 Fabrication of Cf/Ni-EVA composites

The optical image of the fabricated neat EVA polymer, 0.5 wt% Cf/EVA, 0.5 wt% Cf_t/EVA and 0.5 wt% Cf/Ni-EVA composite samples at 147 °C are displayed in (the Supplementary Fig. S1a–d). It was observed from the results that the carbon fibers were homogeneously distributed with a random orientation and bundle aggregates formed to some extent in the EVA polymer matrix of the untreated 0.5 wt% Cf/EVA composite (Supplementary Fig. S1b) than the heat treated 0.5 wt% Cf_t/EVA composite (Supplementary Fig. S1c). The reinforcement of the EVA polymer by the carbon fibers provided reinforcing and bulking effects to the produced polymer composite. The untreated, heat treated and nickel coated carbon fibers can work as strengthening reinforcement fibers, linking the EVA polymer matrix in which they are embedded in, and therefore, imparting high reinforcement effect. It was also observed that the 0.5 wt% Cf/Ni-EVA has lower extent of formation of such agglomerated bundles (Supplementary Fig. S1d) and are more homogeneously distributed than the heat treated 0.5 wt% Cf_t/EVA (Supplementary Fig. S1c) and the untreated 0.5 wt% Cf/EVA one (Supplementary Fig. S1b). In addition, the nickel coated carbon fibers and the heat treated one have stronger binding with the EVA polymer matrix than the untreated carbon fibers [57, 58]. The distribution of the carbon fibers in the composite was mostly homogeneous, and their arrangement in the matrix did not demonstrate any orientation. The lack of fiber orientation is specific to the composite production techniques. It can be also noticed that small parts of carbon fibers protrude from the matrix's surface. The fibers have therefore, been broken. This indicates an increased EVA–fiber interaction. The different lengths of protruding

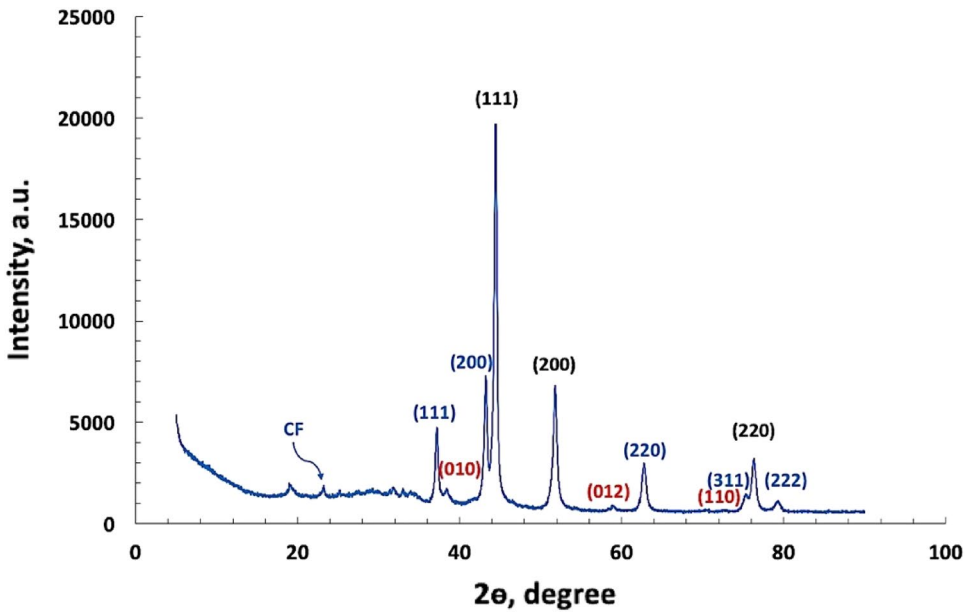

Fig. 7 XRD pattern of the prepared 10wt% Cf/Ni nanocomposites by the electroless deposition method

fiber parts indicate a non-homogeneous adherence between the fibers and the EVA polymer.

3.4 Thermogravimetric analysis

The TGA profile of weight loss as a function of temperature of the carbon fibers as well as the EVA samples are shown in Fig. 8a. It was observed from the results that the carbon fibers are thermally stable and a few decline in the curve at 480 °C of 20 wt% loss at 1000 °C. This weight loss can be expected due to the dissociation of the organic binding agent which added during the manufacture process of the carbon fibers. However, in case of the neat EVA sample; two thermal decomposition stages pathway with the first step attributed to the decomposition of vinyl acetate groups (deacetylation) by the elimination of acetate side acetoxy groups and the subsequent loss of acetic acid, leaving behind them an unsaturated polyene polymer of carbon–carbon double bonds backbone [59]. The wt% loss after the first degradation step was a qualitative index of the amount of vinyl acetate in the copolymer. In this work, the obtained value was about 25 wt%. While the second step is attributed to random chain scission which forms unsaturated volatile species like butane and ethylene reach full thermal decomposition by raising the temperatures [59]. Then, the neat EVA sample was almost completely decomposed by two-step degradation process at 280–360 °C by 38 weight loss % at 345 °C T_{max1} and at 360–480 °C with 467 °C T_{max2} as shown from the derivative thermogravimetric analyses in Fig. 7b. On the other hand, the TGA profiles of Cf/Ni-EVA is similar to the neat EVA however, the T_{max1} and T_{max2} values are found 351 °C and 472 °C higher than the neat EVA as shown from

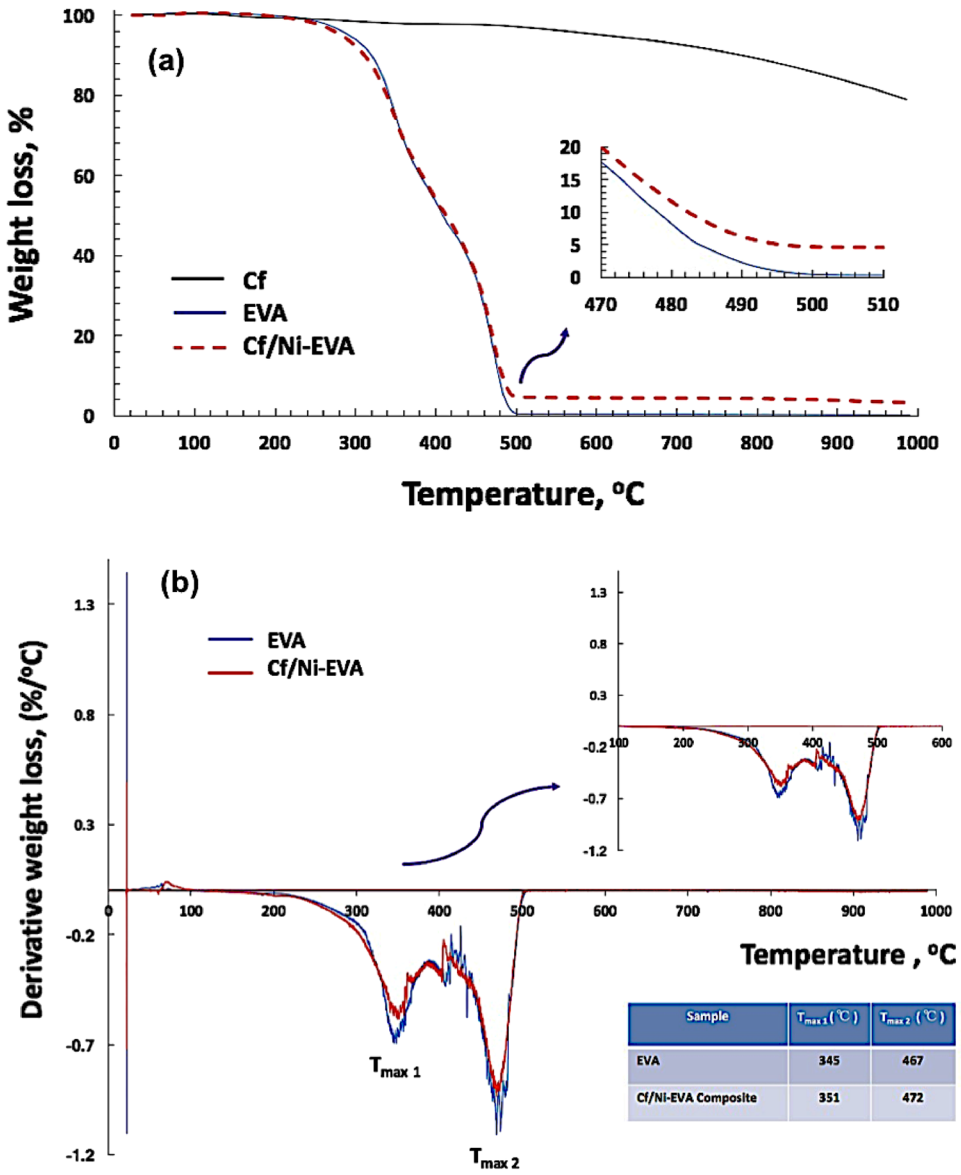

Fig. 8 **a** Thermogravimetric (TGA) and **b** derivative thermogravimetric analyses of the carbon fibers, neat EVA polymer and the prepared Cf/Ni-EVA composites

the derivative thermogravimetric analyses in Fig. 7b due to the combination between the 10 wt% nickel coated carbon fibers with the EVA matrix in the Cf/Ni-EVA composites. It was revealed that, the impregnation of the nickel coated carbon fibers improve the thermal stability of the EVA polymer and can be expected to protect the EVA molecules from the attack of the oxidation at this temperature. It also indicates that, the addition of the nickel coated carbon fibers improve the interfacial bonding in the EVA matrix resulting delayed of volatilization of the polymer chains. A significant influence of the nickel coated carbon fibers on the crystallization behavior, therefore suggesting that, the crystallization of ethylene segments is affected by the interaction of the nickel nanoparticles with nearby vinyl acetate units. Therefore, it also affects the mobility of the crystallize ethylene sequences located in its vicinity. Several studies demonstrated that the EVA chain structure essentially consists of isolated vinyl acetate units and randomly distributed among longer ethylene sequences. The following scheme illustrate the expected thermal decomposition mechanism of the neat EVA sample [60, 61].

$$-\left[CH_2CH_2\right]_n-\left[CH_2CHOCOCH_3\right]_m \xrightarrow{300-400\,^{\circ}C} nCH_3-COOH + -\left[CH_2CH_2CH=CH\right]_n- \quad (6)$$

$$-\left[CH_2CH_2CH=CH\right]_n- \xrightarrow{400-500\,^{\circ}C} \text{Hydrocarbons} \quad (7)$$

3.5 Electrical resistivity of carbon fibers/Ni nanocomposites

The electrical resistivity of the carbon fibers/Ni nanocomposites was measured to study the correlation between the bonding and the adhesion of the deposited nickel layer on the surface of the carbon fibers. A higher void content at measuring the contact electrical resistivity of the carbon fiber/Ni interfaces which would result higher contact resistivity indicating lower adhesion. When measuring the resistivity of the uncoated and Ni-coated fibers, as shown in Fig. 9, it was found that, the electrical resistivity of the untreated carbon fiber itself is higher than the resistivity of the nickel coated carbon fibers fabricated by the electroless deposition. This was probably due to the deposition of high purity metallic nickel layer on the surface of the carbon fibers which enhance the interfacial adhesion between carbon fibers leading to improve the electrical conductivity and decrease the resistivity. However, the heat-treated carbon fibers have the lower resistivity value. It can be expected that the reason behind the higher resistivity of the nickel coated carbon fibers than the heat treated one is due to the functionalization

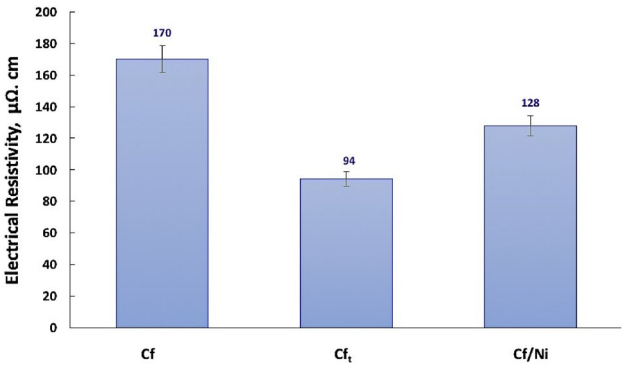

Fig. 9 Electrical resistivity values of the investigated carbon fibers, heat treated and its Ni composite

process by nitric acid which brake the –C=C bond system and decrease and impede the mobility of the p_z electrons of the carbon atoms and decreasing the conductivity [50, 62, 63]. Also, the electrical resistivity of the prepared neat EVA as well as the 0.5 wt% Cf-EVA composite were measured. It was revealed that the electrical resistivity of the neat EVA is decreased from 3.2×10^{10} to 1.4×10^{4} Ω cm in case of 0.5 wt% Cf/Ni-EVA. It was expected that, the coating of the carbon fibers with nickel improve the electrical properties of the EVA polymer matrix composites. In the carbon fibers reinforced by polymer matrix composites, the adequate bonding between Cfs and polymer matrix guarantees the excellent performance of the composites. The higher the interface bonding strength between Cfs and polymer matrix in the composites, the more conductivity and the properties of the obtained composites will be improved. Table 2 lists the values of the electrical resistivity in comparison with similar materials of previous work reported in the literature.

3.6 Mechanical properties of carbon fibers/Ni-EVA composites

In the tensile test of carbon fibers reinforced polymer matrix composites, the properties were varying by the changing in the surface properties and the volume % of Cfs in the (EVA) polymer. The improvements of the surface properties as well as the interfacial adhesion between the Cfs and the polymer matrix are significantly enhancing the mechanical properties of the carbon fibers reinforced with polymer composites [67]. Because the interface is an important factor can affect on the performance of the composite materials, good bonding and adhesion at the interface is essential to achieve the strength of the carbon fibers reinforced the polymer matrix composites [68]. It was also reported in previous work that the homogeneous distribution of particles, such as fibers and platelets, in the polymer matrix improves the mechanical

Table 2 Properties of reinforced EVA polymer matrix composites

Composition	Fabrication method	T_{max1}, °C	T_{max2}, °C	Electrical resistivity Ω cm	Tensile strength, MPa	Young's modules, MPa	Ultimate elongation %	Elongation at break %	References
EVA	Melting	345	467	3.2×10^{10}	–	15.94	366	242	Current work
Cf/Ni-EVA	Melt blending	371	472	1.4×10^{4}	–	24.35	500	180	Current work
Cf/EVA	Hot pressing	–	–	5.99×10^{-2}	24	–	–	1.5	[64]
Biochar fibers/EVA	Melt-mixing	351	475	1×10^{2}	–	87.8	–	240.5	[65]
CNT/EVA	Melt blending using a counter-rotating	351	473	19×10^{5}	–	5.25	–	425	[66]

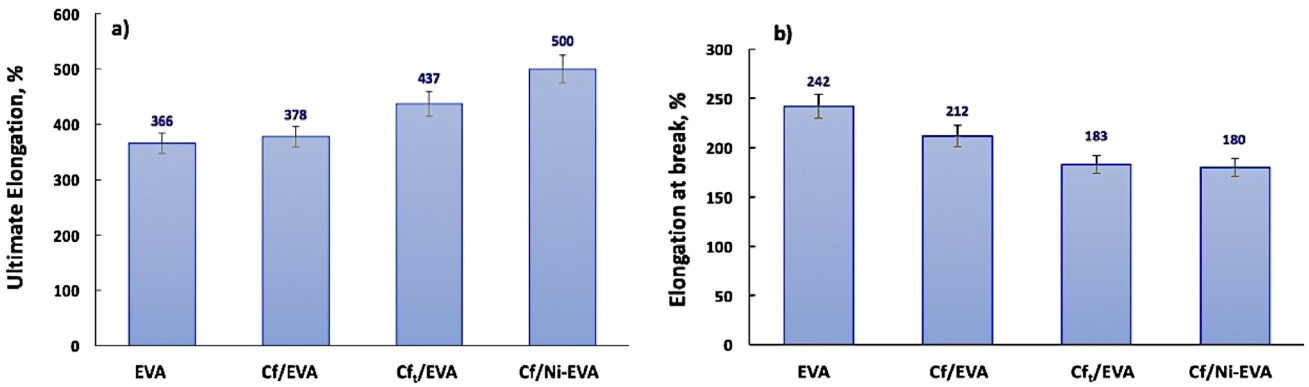

Fig. 10 **a** Ultimate elongation and **b** elongation at break of the fabricated pure EVA polymer, 0.5 wt% Cf/EVA, 0.5wt % Cf$_t$/EVA and 0.5 wt% Cf/Ni-EVA composites samples

stiffness of the fibers through the Exfoliation mechanism [69]. A good surface affinity between EVA and the carbon fibers and the very large surface area for the interaction of stiff carbon fibers with the polymer chains are not enough to achieve exfoliation prior break-up and a surface coating of the carbon fibers is required and a large interfacial area for interaction between polymer chains and the carbon fibers is thus created. To date, the preparation of fully exfoliated EVA-nanocomposites remains a challenge [69]. The results of the ultimate elongation and elongation at break for the prepared polymer composite materials are presented in Fig. 10a, b. It was observed from the results that the ultimate elongation of the EVA is increased by reinforcing the EVA polymer with 0.5 wt% of carbon fibers. Also, the carbon fibers/Ni-EVA Composites exhibited the highest value among all the produced composite samples with an ultimate elongation of 500%. However, the elongation at break of the carbon fibers/Ni-EVA Composites has lowest elongation at break due to the effect of combination with the carbon fibers reinforcements in the EVA polymer matrix decreasing the ductility of the Composites. Figure 11 represents the values of the Young's modulus of the produced composites. It was revealed that; the heat treatment as well as the

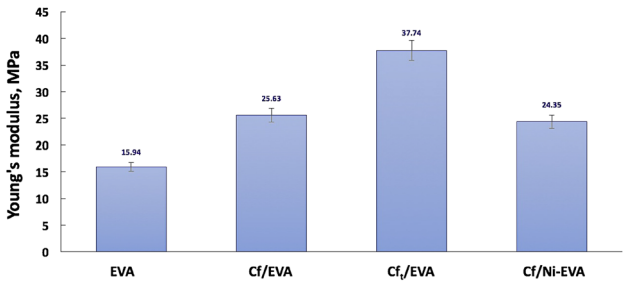

Fig. 11 Young's modulus of the fabricated pure EVA polymer, 0.5 wt% Cf/EVA, 0.5 wt% Cf$_t$/EVA and 0.5 wt% Cf/Ni-EVA composites samples

acid functionalization and nickel coating processes of carbon fibers had enhance the tensile properties. The Young's modulus of the EVA polymer was increased by reinforcing with the carbon fibers and the highest value is observed in the composite sample reinforced with the heat-treated fibers (0.5 wt% Cf$_t$/EVA). However, the produced Cf/Ni-EVA polymer composite has lower Young's modulus than the Cf$_t$/EVA. It may be due to the effect of the functionalization process which can effect on the –C=C-bonding in the graphitic

structure of the carbon fibers. It was reported in the literature that improving the interface properties between polymer matrix and Cfs, can be achieved by increasing the roughness of Cfs surface or depositing an interlayer or adhered coating layer on Cfs surface, both of which are currently considered effective. However, the interfacial bonding strength is not the best solution, because increasing the interfacial bonding strength can quickly reduce the composites' toughness [70]. By using EVA, it was possible to achieve good distribution of carbon fibers in the polymer matrix. Reasonable improvements of the tensile properties were identified, which was due to the isotropic distribution of the carbon fibers in the EVA polymer matrix, adhesion, and wettability, but also an opposite effect can be expected due to the presence of carbon fibers aggregates which acted as a discontinuity of the composite structure [71, 72]. Table 2 lists the different values of the tensile properties in comparison with similar materials of previous work reported in the literature.

The bridging and the pulling-out of carbon fibers at fractured zones of the composite specimen can be shown in Fig. 12. It is attributed to the fact that the occurrence of a bridging mechanism is because of the better adhesion of the carbon fibers with the EVA polymer matrix. The magnified optical images of the fiber–matrix interface (Fig. 12b–d) demonstrates the presence of carbon Cfs along the matrix. The Cfs junctions at the interface with the EVA polymer matrix demonstrates no clear crack formation, which indicates good wettability when compared to the EVA matrix (Fig. 12a). The optical image also demonstrates the presence of a nickel coated fiber–matrix interface, which likely derives from the addition of the EVA as an adhesive agent (Fig. 12d). In addition, the nickel nanoparticles deposited on the fiber's surface increase the fiber's roughness, thereby improving its adherence to the EVA matrix (better anchoring in the EVA). A similar interface microstructure was observed in previous work of Cf/epoxy polymer matrix composites [71, 72].

4 Conclusion

The work provides an overview on the processing technique that have been developed for fabricating carbon fibers-metal/polymer composites. New stretchable and conductive carbon fibers/nickel-EVA composites were prepared by melt blending using untreated, heat treated and functionalized nickel coated carbon fibers. Alkaline hydrazine bath was used as an autocatalytic electroless deposition process of nickel on the surface of the acid treated (functionalized) carbon fibers. Carbon fibers underwent heat treatment and acid functionalization with HNO_3 before coating with nickel. Thin layer of nickel nanoparticles were successfully deposited and completely encapsulated the surface of the acid treated carbon fibers. The electrical resistivity of the produced carbon fibers/Nickel composite is lower than the untreated one. However, the heat-treated carbon fibers have lower electrical resistivity than the nickel coated one due to the acid treatment and the electroless nickel deposition process which change the surface properties of the graphitic structure of the treated carbon fibers and resist the electron movements. The obtained treated and nickel coated carbon fibers were reinforced in EVA polymer by melt blend technique. The thermal stability of EVA was improved by the impregnation of the nickel coated carbon fibers in the EVA polymer matrix.

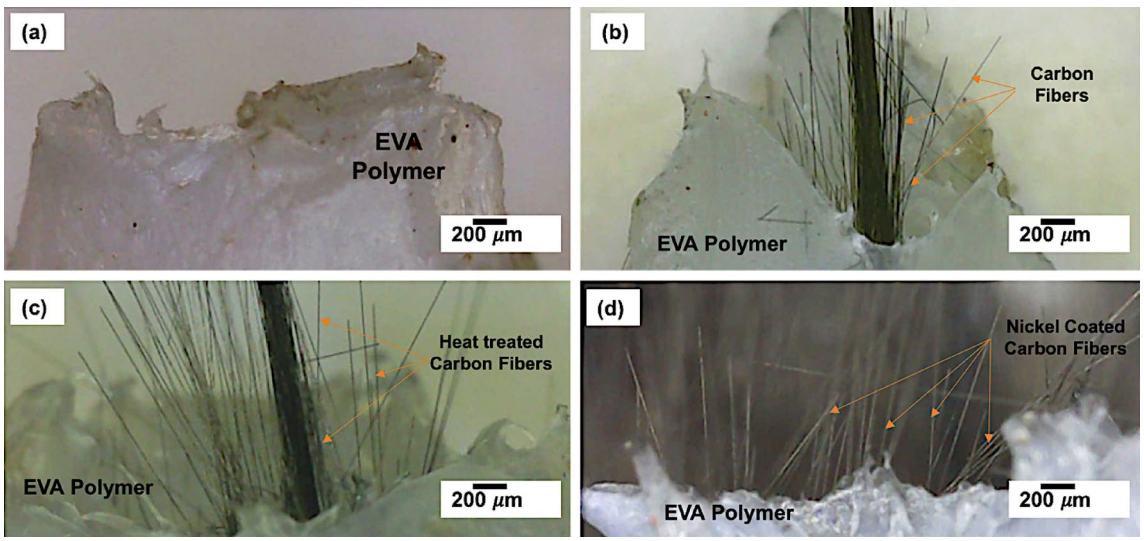

Fig. 12 Optical images of the fracture surfaces of the fabricated **a** pure EVA polymer, **b** 0.5 wt% Cf/EVA, **c** 0.5 wt% Cf_t/EVA and **d** 0.5 wt% Cf/Ni-EVA composites samples

The ultimate elongation as well as the Young's modulus of the prepared EVA samples were improved by reinforcing the EVA polymer with the carbon fibers. Also, the ultimate elongation of the neat EVA was increased by reinforcing with 0.5 wt% carbon fibers, however, the carbon fibers/Ni-EVA composites has the best ultimate elongation of 500 % among the samples. On the other hand, the composite sample reinforced with the heat-treated fibers (0.5 wt% Cf_t/EVA) has the best value of Young's modulus, however, the Cf/Ni-EVA polymer composite has lower value than the heat-treated fibers (0.5 wt% Cf_t/EVA) which is due to the effect of the acid functionalization of carbon fibers. Combination of the obtained treated carbon fibers as well as the carbon fibers/Ni composite with EVA polymer matrix resulted in formation of a new type of stretchable conductive polymer composites of good thermal stability. Further research will be focused on developing methods of modifying the surface of the carbon fibers to improve its mechanical, magnetic and electrical properties. Also, the electromagnetic interference applications of the carbon fibers/Ni composite will be extensively study.

Supplementary Information The online version contains supplementary material available at https://doi.org/10.1007/s42823-023-00630-z.

Acknowledgements The authors extend their appreciation to the Deanship of Scientific Research at Imam Mohammad Ibn Saud Islamic University (IMSIU) for funding and supporting this work through Research Partnership Program No. RP-21-09-72.

Author contributions Conceptualization, WMD, AFA, MSS and FI; methodology, WMD, AFA, MSS and FI; validation, WMD, AFA, MSS and FI; formal analysis, WMD, AFA, MSS and FI; investigation, WMD, AFA, MSS and FI; resources, WMD; data curation, WMD, AFA, MSS and FI; writing—original draft preparation WMD; writing—review and editing, WMD, AFA, MSS and FI; visualization, WMD, AFA, MSS and FI supervision, WMD and FI; project administration, WMD All authors have read and agreed to the published version of the manuscript.

Funding The authors extend their appreciation to the Deanship of Scientific Research at Imam Mohammad Ibn Saud Islamic University (IMSIU) for funding and supporting this work through Research Partnership Program no RP-21-09-72.

Declarations

Conflict of interest All authors declare that they have no conflict of interest.

References

1. Kim KW, Kim DK, Kim BS, An KH, Park SJ, Rhee KY et al (2017) Cure behaviors and mechanical properties of carbon fiber-reinforced nylon6/epoxy blended matrix composites. Compos Part B Eng 112:15–21
2. Park SJ (2018) History and structure of carbon fibers. In: Carbon fibers. Springer Series in Materials Science, p 210
3. Hung P, Lau K, Fox B, Hameed N, Lee J, Hui D (2018) Surface modification of carbon fiber using graphene-related materials for multifunctional composites. Compos B Eng 133:240–257
4. Zhang Y, Wang H, Lu H, Li S, Zhang Y (2021) Electronic fibers and textiles: recent progress and perspective. Science 24(7):102716
5. Navalon S, Dhakshinamoorthy A, Alvaro M, Garcia H (2014) Carbocatalysis by graphene-based materials. Chem Rev 114(12):6179–6212
6. Rane A, Thomas S (2018) Methods for synthesis of nanoparticles and fabrication of nanocomposites. Synth Inorgan Nanomater 2018:121–139
7. Lee P, Chen D, Pui D (2003) Experimental study of a nanoparticle virtual impactor. J Nanopart Res 5:269–280
8. Sun L, Mao J, Pan Z et al (1999) Growth of straight nanotubes with a cobalt–nickel catalyst by chemical vapor deposition. Appl Phys Lett 74(5):644–646
9. Daoush WM, Alkhuraiji TS, Khamis MA et al (2020) Microstructure and electrical properties of carbon short fiber reinforced copper composites fabricated by electroless deposition followed by powder metallurgy process. Carbon Lett 30:247–258
10. Daoush WM, Albogmy TS, Khamis MA, Inam F (2020) Syntheses and step-by-step morphological analysis of nano-copper-decorated carbon long fibers for aerospace structural applications. Crystals 10:1090
11. Sayam A, Rahman ANMM, Rahman M, Smriti SA, Ahmed F, Rabbi MF, Hossain M, Faruque MO (2022) A review on carbon fiber-reinforced hierarchical composites: mechanical performance, manufacturing process, structural applications and allied challenges. Carbon Lett 32:1173–1205
12. Irina M, Azmi A, Tan C, Lee C, Khalil A (2015) Evaluation of mechanical properties of hybrid fiber reinforced polymer composites and their architecture. Proc Manuf 2:236–240
13. Tehrani M, Boroujeni A, Hartman T, Haugh T, Case S, Al-Haik M (2013) Mechanical characterization and impact damage assessment of a woven carbon fiber reinforced carbon nanotube–epoxy composite. Compos Sci Technol 75:42–48
14. Lin G, CINTE21 (2022) Global carbon fiber composites market report. Text Sci Res Z1:46–66
15. Zheng H, Zhang W, Li B, Zhu J, Wang C, Song G, Wu G, Yang X, Huang Y, Ma L (2022) Recent advances of interphases in carbon fiber-reinforced polymer composites: a review. Compos Part B Eng 233:109639
16. Zakaria MR, Md Akil H, Abdul Kudus MH, Ullah F, Javed F, Nosbi N (2019) Hybrid carbon fiber-carbon nanotubes reinforced polymer composites: a review. Compos Part B Eng 176:107313
17. Lamorinière S, Jones MP, Ho K, Kalinka G, Shaffer MSP, Bismarck A (2022) Carbon nanotube enhanced carbon fibre-poly(ether ether ketone) interfaces in model hierarchical composites. Compos Sci Technol 221:109327
18. Yousefi N, Fisher SJ, Burgstaller C, Shaffer MSP, Bismarck A (2022) Hierarchical carbon fiber composites incorporating high loadings of carbon nanotubes. Compos Sci Technol 222:109369
19. Hu Y, Wei Y, Han G, Zhang J, Sun G, Hu X, Cheng F (2022) Comparison of impact resistance of carbon fibre composites with multiple ultra-thin CNT, aramid pulp, PBO and graphene interlayers. Compos Part A Appl Sci Manuf 155:106815
20. Pawlik M, Le H, Lu Y (2019) Effects of the graphene nanoplatelets reinforced interphase on mechanical properties of carbon fibre reinforced polymer—a multiscale modelling study. Compos Part B Eng 177:107097
21. Sánchez-Romate XF, Del Bosque A, Artigas-Arnaudas J, Muñoz BK, Sánchez M, Ureña A (2021) A proof of concept of a structural supercapacitor made of graphene coated woven carbon fibers: EIS study and mechanical performance. Electrochim Acta 370:137746

22. Wu Y, Wang LX, Xu H, Wang S, Peng L, Zheng Z et al (2021) Preparation of silver-plated carbon nanotubes/carbon fiber hybrid fibers by combining freeze-drying deposition with A sizing process to enhance the mechanical properties of carbon fiber composites. Compos Part A Appl Sci Manuf 146:106421
23. Liu L, Du M, Liu F (2023) Recent advances in interface microscopic characterization of carbon fiber-reinforced polymer composites. Front Mater 10:1124338
24. Tang Z, He C, Tian H, Ding J, Hsiao BS, Chu B, Chen X (2016) Polymeric nanostructured materials for biomedical applications. Prog Polym Sci 60:86–128
25. Okubo M, Tahara M, Kurok T, Hibimo T, Saeki N (2008) Plating technology for fluorocarbon polymer films using atmospheric-pressure nonthermal plasma graft polymerization. J Photopolym Sci Technol 21:219–224
26. Daoush W, Imae T (2015) Fabrication of PtNi bimetallic nanoparticles supported on multi-walled carbon nanotubes. J Exp Nanosci 10(5):392–406
27. Daoush W, Lim B, Nam D, Hong S (2014) Microstructure and mechanical properties of CNT/Ag nanocomposites fabricated by spark plasma sintering. J Exp Nanosci 9(6):588–596
28. Sun X, Gutierrez A, Yacaman MJ, Dong X, Jin S (2000) Investigations on magnetic properties and structure for carbon encapsulated nanoparticles of Fe Co, Ni. Mater Sci Eng A 286(1):157–160
29. Daoush W, Elkady O (2014) Microstructure, physical properties and hardness of Al_2O_3 short fibres/Ni matrix composites fabricated by powder technology. J Compos Mater 48(30):3735–3746
30. Cai Y, Hu Y, Song L, Lu H, Chen Z, Fan W (2006) Preparation and characterizations of HDPE–EVA alloy/OMT nanocomposites/paraffin compounds as a shape stabilized phase change thermal energy storage material. Thermochim Acta 451:44–51
31. Horrocks A, Price D (2001) Fire retardant materials. Woodhead Publishing, London
32. Duquesne S, Le Bras M, Bourbigot S, Delobel R, Camino G, Eling B, Lindsay C, Roels T, Vezin H (2001) Mechanism of fire retardancy of polyurethanes using ammonium polyphosphate. J Appl Polym Sci 82:3262–3274
33. Huang G, Yang J, Gao J, Wang X (2012) Thin films of intumescent flame retardant–polyacrylamide and exfoliated graphene oxide fabricated via layer-by-layer assembly for improving flame retardant properties of cotton fabric. Ind Eng Chem Res 51(38):12355–12366
34. Jyoti J, Kumar A, Dhakate S, Singh BP (2018) Dielectric and impedance properties of three-dimension graphene oxide–carbon nanotube acrylonitrile butadiene styrene hybrid composites. Polym Testing 68:456–466
35. Jamali AR, Bhatti J, Khan W, Akther F, Batool M, Batool R, Daoush WM (2022) Synthesis and characterization of silver nanoparticle–polydimethylsiloxane (Ag-NP-PDMS) stretchable conductive nanocomposites. Crystals 12(8):1098
36. Wang Z, Zhao GL (2013) Microwave absorption properties of carbon nanotubes-epoxy composites in a frequency range of 2–20 GHz. Open J Compos Mater 3(2):17–23
37. Chrissafis K, Bikiaris D (2011) Can nanoparticles really enhance thermal stability of polymers? Part I: an overview on thermal decomposition of addition polymers. Thermochim Acta 523(1–2):1–24
38. Chung DD (2001) Electromagnetic interference shielding effectiveness of carbon materials. Carbon 39:279–285
39. Singh B, Singh D, Mathur R et al (2008) Influence of surface modified MWCNTs on the mechanical, electrical and thermal properties of polyimide nanocomposites. Nanoscale Res Lett 3:444–453
40. Li M, Feng Y, Wang J (2023) Asymmetric conductive structure design for stabilized composites with absorption dominated ultra-efficient electromagnetic interference shielding performance. Compos Sci Technol 236:110006
41. Yang S, Chen CY, Parng SH (2002) Effects of conductive fibers and processing conditions on the electromagnetic shielding effectiveness of injection molded composites. Polym Compos 23(6):1003–1013
42. Oehler D, Seegert P, Wetzel T (2021) Modeling the thermal conductivity of porous electrodes of Li-ion batteries as a function of microstructure parameters. Energ Technol 9:2000574
43. Abdel Rafea M, Eid A, Daoush W (2023) Synthesis and characterization of carbon nanotube/copper oxide nanocomposite as an enhanced absorber for solar radiation. Opt Mater 138:113643
44. Wang C, Wan W, Huang Y (2014) Hierarchical MoS_2 nanosheet/active carbon fiber cloth as a binder-free and free-standing anode for lithium-ion batteries. Nanoscale 6:5351–5358
45. Tadjine R, Houimi A, Alim M, Oudini N (2022) Oxygen flow rate effect on copper oxide thin films deposited by radio frequency magnetron sputtering. Thin Solid Films 741:139013
46. Murali D, Kumar S, Choudhary R, Wadikar A, Jain M, Subrahmanyam A (2015) Synthesis of Cu_2O from CuO thin films: optical and electrical properties. AIP Adv 5:047143
47. Ribeiro Y, Pereira J, David D, da Silv M (2022) Growth, characterization, and photovoltaic application of copper oxide thin films. Thin Solid Films 757:139381
48. Chevallier C, Bose S, Hamady S, Horwat D, Pierson J, Boulet P, Fressengeas N (2022) Effect of temperature and D-sorbitol reducing agent content on the structural and optical properties of copper oxide thin films deposited by ultrasonic spray pyrolysis. Thin Solid Films 758:139435
49. Abdel Rafea M, Roushdy N (2009) Determination of the optical band gap for amorphous and nanocrystalline copper oxide thin films prepared by SILAR technique. J Phys D Appl Phys 42:015413
50. Daoush W, Lim B, Mo C, Nam D, Hong S (2009) Electrical and mechanical properties of carbon nanotube reinforced copper nanocomposites fabricated by electroless deposition process. Mater Sci Eng 513–514:247–253
51. Geeth M, Maury M, Al-Maadeed S, Muthalif A, Sadasivuni K (2022) High-precision nonenzymatic electrochemical glucose sensing based on CNTs/CuO nanocomposite. J Electron Mater 51:4905–4917
52. Zhang X, Fan X, Yan C (2012) Interfacial microstructure and properties of carbon fiber composites modified with graphene oxide. ACS Appl Mater Interfaces 4:1543–1552
53. Feng M, Wang S, Yu Y, Feng Q, Yang J, Zhang B (2017) Carboxyl functionalized carbon fibers with preserved tensile strength and electrochemical performance used as anodes of structural lithium-ion batteries. Appl Surf Sci 392:27–35
54. Schlesinger M (2000) Electroless deposition of nickel. Modern Electroplat 4:667–684
55. García-Cerda LA, Bernal-Ramos KM, Montemayor SM, Quevedo-López MA, Betancourt-Galindo R, Bueno-Báques D (2011) Preparation of hcp and fcc Ni and Ni/NiO nanoparticles using a citric acid assisted pechini-type method. J Nanomater 2011:162495
56. Eluri R, Paul B (2012) Synthesis of nickel nanoparticles by hydrazine reduction: mechanistic study and continuous flow synthesis. J Nanopart Res 14:800
57. El-Sabbagh SH, Ahmed NM, Daoush W (2006) Colored rubber vulcanizates with some magnetic properties. J Appl Polym Sci 102:494–505
58. Mansour SH, Ahmed NM, Daoush W (2007) Studies on magnetic pigmented polyester composites. Polym Plast Technol Eng 46:85–96
59. Maria HJ, Lyczko N, Nzihou A et al (2013) Transport of organic solvents through natural rubber/nitrile rubber/organically modified

montmorillonite nanocomposites. J Mater Sci 48:5373–5386. https://doi.org/10.1007/s10853-013-7332-7
60. Costache MC, Jiang DD, Wilkie CA (2005) Thermal degradation of ethylene–vinyl acetate coplymer nanocomposites. Polymer 46(18):6947–6958. https://doi.org/10.1016/j.polymer.2005.05.084
61. Sobhy M et al (2022) Thermal properties of nano tungsten-ethylene vinyl acetate (EVA) composites. 2020 IOP Conf Ser Mater Sci Eng 975:012003
62. Daoush WM, Imae T (2012) Syntheses and characterizations of multi-walled carbon nanotubes-supported palladium nanocomposites. J Mater Res 27(13):1680–1687
63. Daoush WM, Hong SH (2013) Synthesis of multi-walled carbon nanotube/silver nanocomposite powders by chemical reduction in aqueous solution. J Exp Nanosci 8(5):578–587
64. Lu H, Li Z, Qi X, Xu L, Chi Z, Duan D, Islam MDZ, Wang W, Jin X, Zhu Y, Fu Y, Cui L, Zhuang Y, Dong Y (2021) Flexible, electrothermal-driven controllable carbon fiber/poly(ethylene-co-vinyl acetate) shape memory composites for electromagnetic shielding. Compos Sci Technol 207:108697
65. Faga MG, Duraccio D, Di Maro M, Pedraza R, Bartoli M, d'Ayala GG, Torsello D, Ghigo G, Malucelli G (2022) Ethylene-vinyl acetate (EVA) containing waste hemp-derived biochar fibers: mechanical, electrical, thermal and tribological behavior. Polymers 14:4171. https://doi.org/10.3390/polym14194171
66. Zubkiewicz A, Szymczyk A, Franciszczak P, Kochmanska A, Janowska I, Paszkiewicz S (2020) Comparing multi-walled carbon nanotubes and halloysite nanotubes as reinforcements in EVA nanocomposites. Materials 13:3809. https://doi.org/10.3390/ma13173809
67. Gan X (2009) Effect of interface structure on mechanical properties of advanced composite materials. Int J Mol Sci 10(12):5115–5134
68. He D, Fan B, Zhao H, Lu X, Yang M, Liu Y et al (2017) Design of electrically conductive structural composites by modulating aligned CVD-grown carbon nanotube length on glass fibers. ACS Appl Mat Interfaces 9(3):2948–2958
69. Pasanovic-Zujo V, Gupta RK, Bhattacharya SN (2004) Effect of vinyl acetate content and silicate loading on EVA nanocomposites under shear and extensional flow. Rheol Acta 43(2):99–108
70. Adams JB, Wolfer WG, Foiles SM (1989) Elastic properties of grain boundaries in copper and their relationship to bulk elastic constants. Phys Rev B 40(14):9479–9484
71. Kamae T, Drzal LT (2022) Carbon fiber/epoxy composite property enhancement through incorporation of carbon nanotubes at the fiber-matrix interphase—part II: mechanical and electrical properties of carbon nanotube coated carbon fiber composites. Compos Part A Appl Sci Manuf 160:107023
72. Sinha Ray S, Okamoto M (2003) Polymer/layered silicate nanocomposites: a review from preparation to processing. Progr Polym Sci (Oxf) 28(11):1539–1641

Authors and Affiliations

Walid M. Daoush[1,2] Abdullah Fahad Al-Zuair[1] Mohd Shahneel Saharudin[3] Fawad Inam[4,5]

✉ Walid M. Daoush
wmdaoush@imamu.edu.sa

Abdullah Fahad Al-Zuair
Abdullah.188@outlook.sa

Mohd Shahneel Saharudin
s.saharudin@rgu.ac.uk

Fawad Inam
f.inam@uel.ac.uk

[1] Department of Chemistry, College of Science, Imam Mohammad Ibn Saud Islamic University (IMSIU), P.O. Box 90950, 11623 Riyadh, Saudi Arabia

[2] Department of Production Technology, Faculty of Technology and Education, Helwan University, Saray-El Qoupa, El Sawah Street, Cairo 11281, Egypt

[3] School of Engineering, Robert Gordon University, Aberdeen, UK

[4] School of Architecture, Computing and Engineering, University of East London, London, UK

[5] Executive Principal Office, Oxford Business College, 23-38 Hythe Bridge Street, Oxford, OX1 2EP, UK

Supplementary Figure

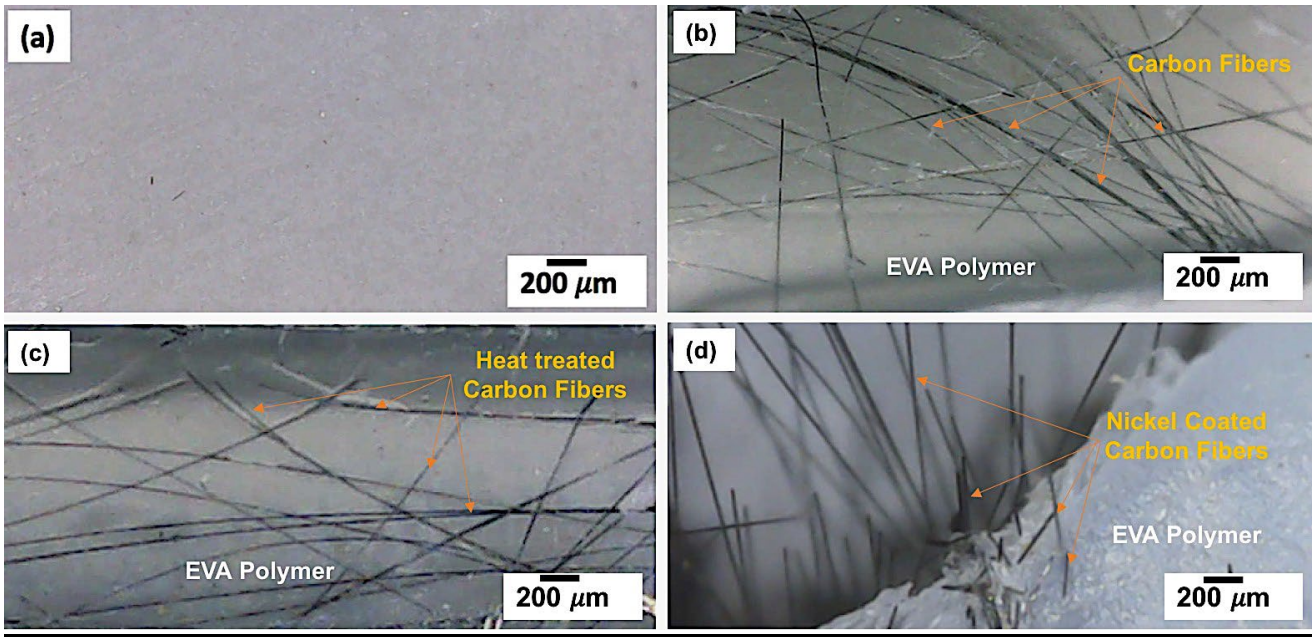

Figure 1 Optical images of the fabricated (a) pure EVA polymer, (b) 0.5 wt % Cf/ EVA, (c) 0.5 wt % Cf_t/EVA and (d) 0.5 wt % Cf/Ni-EVA composites samples.